Simple and Fast Method To Fabricate Single-Nanoparticle-Terminated Atomic Force Microscope Tips

9 AUTHORS, INCLUDING:

Hui-Wen Cheng
National Chiao Tung University
8 PUBLICATIONS   **18** CITATIONS

SEE PROFILE

Yuan-Chih Chang
Academia Sinica
41 PUBLICATIONS   **327** CITATIONS

SEE PROFILE

Fu-Rong Chen
National Tsing Hua University
182 PUBLICATIONS   **3,136** CITATIONS

SEE PROFILE

Fan-Gang Tseng
National Tsing Hua University
326 PUBLICATIONS   **2,491** CITATIONS

SEE PROFILE

Simple and Fast Method To Fabricate Single-Nanoparticle-Terminated Atomic Force Microscope Tips

Hui-Wen Cheng,[†] Yuan-Chih Chang,[§,%] Chi-Tsu Yuan,[⊥] Song-Nien Tang,[#] Chia-Seng Chang,[§] Jau Tang,[∥,∞] Fu-Rong Chen,[†] Rong-Long Pan,[‡] and Fan-Gang Tseng*,[†,∥]

[†]Department of Engineering and System Science and [‡]Department of Life Science, National Tsing Hua University, Hsinchu 30013, Taiwan

[§]Institute of Physics and [∥]Research Center for Applied Sciences, Academia Sinica, Nankang, Taipei 11529, Taiwan

[⊥]Department of Physics, Chung Yuan Christian University, Chungli 32023, Taiwan

[#]Medical Image Technology Department, Industrial Technology Research Institute, Hsinchu 31040, Taiwan

[∞]Institute of Photonics, National Chiao Tung University, Hsinchu 30010, Taiwan

S *Supporting Information*

ABSTRACT: This paper introduces a simple, yet controllable scheme to pick up a single 13 nm Au nanoparticle (Au-NP) using the tip of an atomic force microscope (AFM) probe through the application of electrical biases between the tip and the Au-NP. Transmission electron microscope (TEM) images were acquired to verify that a single Au-NP was attached to the AFM probe. We postulate that the mechanism underlying the ability to manipulate individual Au-NPs at the apex of the AFM probe tip is Coulomb interaction induced by tip bias. The AFM tip with the attached Au-NP was then used to study the interaction between a single quantum dot (QD) and the Au-NP. The blinking behavior of single colloidal CdSe/ZnS core/ shell QD was significantly suppressed with the approach of the 13 nm Au-NP attached to the AFM tip.
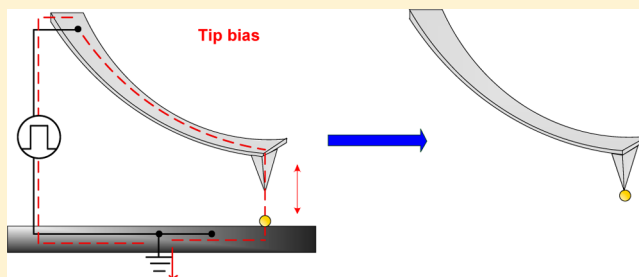
INTRODUCTION

Scanning tunneling microscope (STM)[1] and atomic force microscope (AFM)[2] have revolutionized surface sciences by enabling the study of surface topography and other surface properties at the angstrom-to-micrometer scale. The three major functions of AFM include imaging, force spectroscopy (i.e., obtaining a force−distance curve), and manipulation (nanolithography). AFM techniques employ a very sharp tip as a probe to scan and image surfaces. Spectroscopic information reveals changes in the forces acting on the tip as it approaches and is withdrawn from the surface. As the tip is brought toward the sample, van der Waals forces cause attraction, which increases as the distance is reduced. However, when the separation between the tip and the surface is reduced to only a few micrometers, repulsive forces become dominant, causing the cantilever to bend as the tip is brought closer to the surface. The repulsive force is calculated from Hooke's law: $F = -kd_c$, where k is the spring constant of the cantilever and d_c is the cantilever deflection. Interactions other than repulsive forces and van der Waals forces also affect the tip. When AFM is performed in ambient air, the sample and tip are often coated with a thin layer of fluid (mainly water), resulting in capillary forces when the tip approaches the surface. Xie et al.[3] classified nanolithographic techniques into two groups: force-assisted and bias-assisted nanolithography.

In AFM, the interactive force between the tip of the probe and the sample surface is determined according to the deflection of a microfabricated cantilever with the tip positioned at the free end. Modifying the probe enables researchers to explore a range of surface characteristics. AFM probes with individual microparticles or nanoparticles attached to the cantilever/tip have been widely used to measure surface forces in AFM and near-field scanning optical microscope (NSOM),[4] as the geometry and composition of the particle can be well controlled.

Ducker et al.[5,6] were pioneers in the attachment of microspheres to a tipless AFM cantilever with resin. Their colloidal probe technique employed a laser-pulled micropipet attached to an optical microscope. Mak et al.[7] improved this method through their dual wire technique, in which glue and a microsphere are simultaneously applied to a cantilever using two micropipets. Lantz et al.[8] applied this method to the attachment of FeNdBLa magnetic microparticles to an AFM tip to increase the resolution of magnetic force microscopy. Using a microcolloidal probe, Berdyyeva et al. revealed how the rigidity of human epithelial cells increases with age.[9] Since the 1990s, the microcolloidal probe technique has become one of
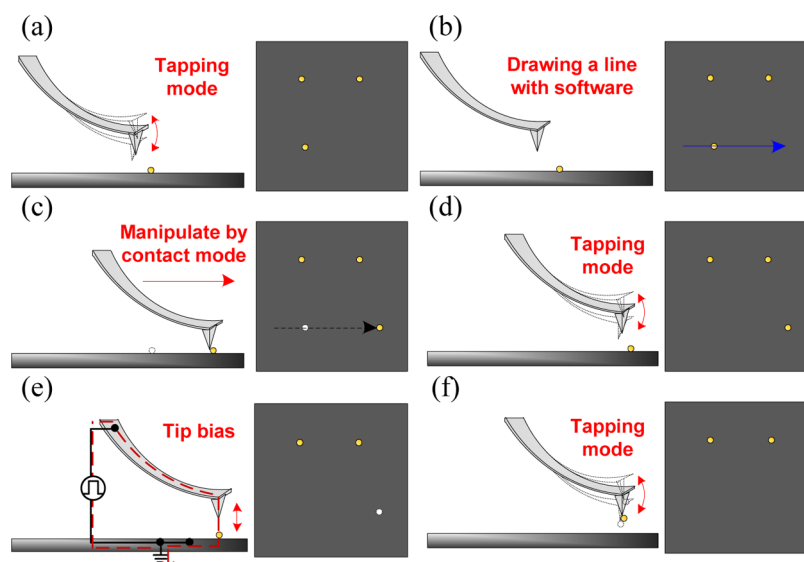
Figure 1. Schematic diagram outlining the procedures used to pick up a single Au-NP with the end of an AFM probe. The parts in the figure are not drawn to scale. (a) First, an image is taken. (b) The tip is positioned behind the selected Au-NP, and a line is drawn across the particle using AFM software. (c) The tip is used to push the Au-NP (in contact mode) along the trajectory of the drawn line. (d) Another image is taken to verify the results of the manipulation. If the Au-NP was not moved to the target position, the manipulation process would be repeated. (e) The probe is moved toward the selected particle (force−distance curve operation) with the tip biased at greater than 4 V to pick up the Au-NP. Because of spatial drift resulting from environmental conditions, this process must be repeated until the tip is positioned exactly above the Au-NP. (f) A final image is taken to verify the success of the Au-NP pick-up operation.

the most popular techniques for the measurement of surface forces, primarily because of the ease of technical application, the ability to directly measure forces generated between the particle and various materials, and a more precise contact area than that afforded by a tipless probe. However, the minimum size of particles that can be attached to the AFM tip is approximately 1 μm,[10] mainly because of the colloidal attachment process involving optical microscopes and the need to perform micromanipulation with limited resolution. Preventing contamination resulting from the adsorption of glue on the surface of the sphere is crucial to successful attachment.[11]

Ong and Sokolov sought to apply this colloidal attachment method to nanoparticles by applying glue to the AFM tip; however, this approach resulted in the attachment of many nanoparticles at once.[12] Vakarelski et al.[13,14] developed a wet-chemistry procedure to attach a single nanoparticle to the vertex of an SPM probe tip. Wang et al.[15] used an electrochemical oxidation−reduction reaction to attach or grow a nanoparticle (14−50 nm) selectively on the tip of an AFM probe. Both of these methods employed self-assembled monolayers (SAMs) as material-selective linkers. Okamoto et al.[16] employed the photocatalytic effect of a semiconducting material (TiO$_2$) to deposit Au nanoparticles (Au-NPs) (ranging in size from 100 to 300 nm) to the tip of an AFM cantilever. Unfortunately, controlling the position and size of these nanoparticles proved to be difficult. Hoshino et al.[17] introduced a nanostamp method to attach sub-10 nm colloidal quantum dots (QDs) arrays to a Si probe; however, the number of QDs could not be effectively controlled.

Eckel et al.[18] and Lee et al.[19] employed an Au-NP-immobilized AFM probe[18] and gold-deposited silica-bead AFM probe[19] to measure and quantify fluorescence emissions as a function of distance between the nanocrystal and the tip. However, their quenching agents were multiple Au-NPs[18] and Au films.[19]

This study outlines the methodology to pick up a single 13 nm Au-NP using an electrically biased AFM tip. The interaction of Coulomb forces induced by the tip bias makes it possible to pick up the Au-NP from the substrate in a controllable manner. This method provides the following benefits: (1) the AFM probes do not require surface pretreatment; (2) Au-NPs of various sizes can be attached (see Supporting Information); (3) the entire process can be completed within 10−15 min. We employed direct transmission electron microscope (TEM) observation and indirect fluorescence photon antibunching inspection to verify our success in picking up a single 13 nm Au-NP. This probe could be of considerable practical value for manipulating individual nanosized objects (such as single molecules) in the future.

■ EXPERIMENTAL METHODS

The following reagents were used throughout the study: 13 nm Au-NP solution (TAN Bead, 179 ppm in H$_2$O), anhydrous ethanol (Sigma-Aldrich, ≥99.5%), 12 nm Qdot 655 ITK organic quantum dots (Invitrogen, 1 μM solution in decane), and decane (Sigma-Aldrich, ≥99%).

This study employed an MFP-3D-BIO AFM (Asylum Research, U.S.), HITACHI S-4800 field emission scanning electron microscope (FE-SEM), JEOL 2000 V UHV-TEM, and MicroTime 200 fluorescence lifetime systems with inverse time-resolved fluorescence microscope (PicoQuant, Germany). For the preparation of samples, we employed 24 mm × 50 mm glass coverslips, Lamda microliter pipettes, and a TR15 spin coating machine. To attach the Au-NPs, we employed standard silicon polygon-pyramidal tips (NanoWorld Pointprobe NCH probes, tip radius of curvature of <12 nm, resistivity of 0.01−0.025 Ω·cm) supported by a cantilever with a spring constant of $k \approx 42$ N/m and silicon polygon-pyramidal tips with PtIr coating (NANOSENSORS PPP-NCHPt probes, tip radius of curvature of <25 nm, electrically conductive) supported by a cantilever with a spring constant of $k \approx 42$ N/m. To support
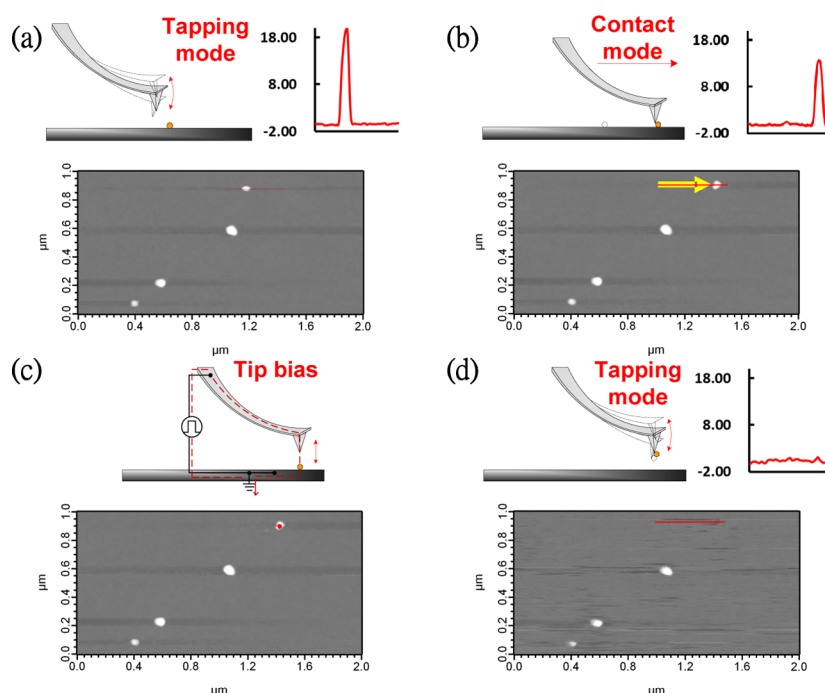
Figure 2. Illustration of AFM probe (with PtIr coating) picking up a 13 nm Au-NP: (a) before pushing the Au-NP to the right, as indicated by the yellow arrow; (b) after pushing the Au-NP; (c) probe is moved toward the Au-NP (force−distance curve operation) (red point) using a tip bias of 4 V; (d) final image showing that the Au-NP has been removed from the surface. A cross-section profile of the red line is presented in the upper-right inset.

the Au-NPs during attachment, we employed conductive n-type polished Si (100) wafers (resistivity of 0.008−0.022 Ω·cm), purchased from Swiftek Corp, Taiwan.

For the experiments in which Au-NPs were picked up, the initial Au-NP solution was diluted with ethanol at a volume ratio of 1:1000. The Au-NPs were spread as a monolayer on a conductive silicon wafer by spin-coating. The substrates were then heated to 100 °C for 2 min to dry. The surface roughness of the silicon wafer had to be sufficiently low (on the order of 100 pm) to enable the imaging of Au-NPs by AFM.

Fluorescence photon antibunching inspection was used to verify the existence of a single Au-NP on the AFM tip. This involved the preparation of a diluted solution of QDs from the initial Qdot 655 solution and decane at a volume ratio of 1:10000. The diluted QDs solution was spread as a monolayer on a glass coverslip by spin-coating, and the prepared sample was then placed on the fluorescence microscope for measurement. To provide excitation, a picosecond diode laser (excitation wavelength λ_{exc} = 467 nm) was focused to a diffraction limited spot using an oil-immersion objective (Olympus, numerical aperture of 1.4). Fluorescence was collected by the same objective and guided to a confocal pinhole to reject out-of focus light. After passing through the pinhole, the fluorescence signal was split, using a dichroic beam splitter, into two beams and filtered using band-pass filters. The fluorescence signal was finally detected using a pair of single-photon avalanche diodes (SPADs). Time-tagged, time-resolved (TTTR) measurements were performed during the experiments. TTTR is a time-correlated single-photon counting (TCSPC) technique used to record all time information associated with every detected photon, including the relative time between the excitation pulse and photon emission as well as the absolute time between the start of the experiment and the emission of photons. In TTTR mode, the TCSPC setup

enables the simultaneous monitoring of the blinking behavior and lifetime of QDs.[20]

RESULTS AND DISCUSSION

Figure 1 presents a schematic diagram depicting the process of picking up a single Au-NP with the end of an AFM probe. First, an image was scanned using the AFM in tapping mode to select the desired Au-NP for manipulation (Figure 1a). AFM software was then used to draw a pseudo-line across the center of the particle on the acquired image (Figure 1b). The AFM tip was then manipulated (in contact mode) to follow the trajectory of this drawn line, thereby pushing the Au-NP from its original position on the surface (Figure 1c). During the pushing process, z feedback was used to ensure that the AFM tip touched the Au-NP without contacting the substrate. There is always a possibility that the Au-NP may roll or slide to a new position on the substrate during manipulation.[21−23] Thus, an AFM system with a high degree of mechanical stability is required. Prior to any attempts at manipulation, sequential images of the samples[23,24] are examined to obtain information regarding spatial uncertainties originating from thermal drift or nonlinearity in the piezo actuators. Following particle manipulation, the samples are imaged again to observe the results of the manipulation (Figure 1d). In the event that the Au-NP was not moved to the target position, the manipulation procedure would be repeated. This procedure is meant to break the bonds holding the Au-NP to local debris and the substrate.

The tip is then moved to the new position (relative to the Au-NP), and the action generally used to collect a single force−distance curve is performed such that the probe approaches the Au-NP with a tip bias greater than 4 V (Figure 1e). The distance between the tip and the Au-NP is set at 10 nm. After succeeding in picking up a single Au-NP, a final image is taken to verify that the target Au-NP is no longer on the surface
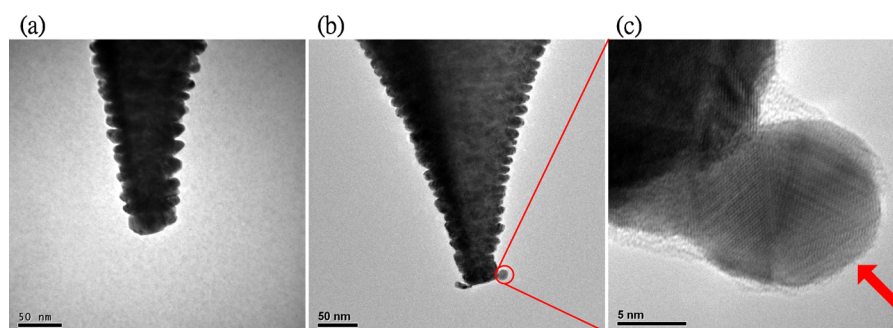
13241

dx.doi.org/10.1021/jp401050t | J. Phys. Chem. C 2013, 117, 13239−13246

Figure 3. (a) TEM image of the apex of a tip prior to the attachment of an Au-NP. (b) AFM probe after picking up a 13 nm Au-NP (scale bar, 50 nm). (c) Magnified image of the right-corner of the apex of the tip in (b) with the red arrow indicating the position of the Au-NP. (scale bar, 5 nm).

(Figure 1f). The spatial resolution of the images is changed because of the shape of the AFM tip with attached Au-NP (see Supporting Information).

To demonstrate the feasibility of this method in picking up a single Au-NP, we performed various experiments using silicon cantilevers in tapping mode. Nonetheless, after many trials (using a batch of six levers), we were unable to obtain any nanoparticle-terminated tips. The failure of these attempts can be attributed to the following: (1) inadequate electrical conduction through the tip of the doped silicon cantilever used to pick up the Au-NP. The low conductivity of the tip also presented charging problems on the TEM images. (2) The silicon tip was easily blunted by stiff objects encountered during the scanning process.[23,25] To overcome these difficulties, we employed silicon cantilevers with PtIr coatings.

AFM images depicting the process of picking up 13 nm Au-NPs are presented in Figure 2. To move an Au-NP to the right, an arrow was drawn to direct the motion of the tip, as shown in Figure 2b. The image obtained after the manipulation (Figure 2b) indicates that the Au-NP was successfully moved to the target position. After the probe was moved toward the selected particle (force−distance curve operation) using a tip bias of 4 V in contact mode (Figure 2c), the particle no longer appeared on the surface, as verified by an image taken in tapping mode (Figure 2d). In the case shown in Figure 2, spatial drift was not significant, as verified by consecutive AFM images.

The proposed system comprises three objects: an AFM probe, an Au-NP, and a substrate plate. Each of these objects is conductive. The Au-NP is first laterally manipulated to a new position. The Au-NPs were spin-coated on the substrate, and the substrate was heated for 2 min to dry in ambient conditions; therefore, a certain amount of contamination existed between the Au-NP and the substrate. This manipulation step is helpful for releasing the Au-NP from bonding to the substrate or surrounding contamination. A voltage is then applied to the AFM probe (4 V), while the voltages of the Au-NP and substrate are held at zero.

Xu et al.[26] observed that a small number of Au-NPs (diameter of ≤2 nm) were picked up, even at zero bias. This was likely due to van der Waals or capillary force interactions between the AFM tip and the Au-NPs on the surface of the substrate. Although it is possible to pick up the Au-NP simply by adhesion interactions, a 13 nm Au-NP could not be picked up without the application of a voltage. These results are consistent with those of Xu.[26]

Takahashi et al.[27,28] used the Johnson−Kendall−Roberts (JKR) model to provide a theoretical estimate of the voltage required to pick up a particle adhered to a substrate.[29] The applied voltage (V) generates an electrostatic force:[27]

$$F_e = \frac{\pi\varepsilon_0}{D/R_{Au\text{-}NP}}V^2 \tag{1}$$

where $R_{Au\text{-}NP}$ is the radius of the Au-NP (13 nm) and D is the distance between the AFM probe and the Au-NP. The distance between the probe tip and the Au-NP was set to 10 nm; therefore, $D = 10$ nm.

The force required to detach the adhered Au-NP from the substrate is expressed as follows:[27]

$$F_a = \frac{3}{2}\pi\Delta\gamma R_{Au\text{-}NP} \tag{2}$$

where $\Delta\gamma$ is the work of adhesion, representing the energy change from the surface to the interface per unit area.[29] For an ideal interface, the work of adhesion is on the order of 1 N/m. $\Delta\gamma$ is seldom equal to or greater than 1. $\Delta\gamma \approx 0.01$ is more common for a surface with a degree of roughness, contamination, or both.[30]

The voltage required to pick up the Au-NP can be obtained from $F_e > F_a$. Therefore, the applied V must be determined as follows:

$$V > \sqrt{\frac{3}{2}\Delta\gamma\frac{D}{\varepsilon_0}} \approx (4.15 \times 10^5)\sqrt{\Delta\gamma D} \tag{3}$$

When $\Delta\gamma$ is approximately equal to 0.01 and D equals 10 nm, the applied V must be greater than 4 V. These calculation results closely match those of our experiments. We suggest that Coulomb interaction is involved in picking up the Au-NP from the substrate.

TEM micrographs of the AFM tip with attached Au-NP were examined to verify the success of picking up the 13 nm Au-NP with the probe. The AFM tip prior to the attachment of an Au-NP (Figure 3a) is shown for comparison. Figure 3b presents an Au-NP attached to the bottom-right corner of the tip apex. HR-TEM was used to reveal the size and shape of the Au-NP through magnification of the image (Figure 3c). The diameter of the Au-NP is approximately 13 nm and a lattice is clearly presented, which confirms that the attached object is indeed an Au-NP.

It is indeed after the pick-up process that all the tips would be terminated with Au-NPs, resulting in a success rate of 100%. This can be verified by checking the remaining Au-NPs on the rescanned AFM image (Figure 2d). However, after TEM imaged the AFM tip under high resolution mode, some Au-NPs on the tip may be damaged by the very focused electron beam
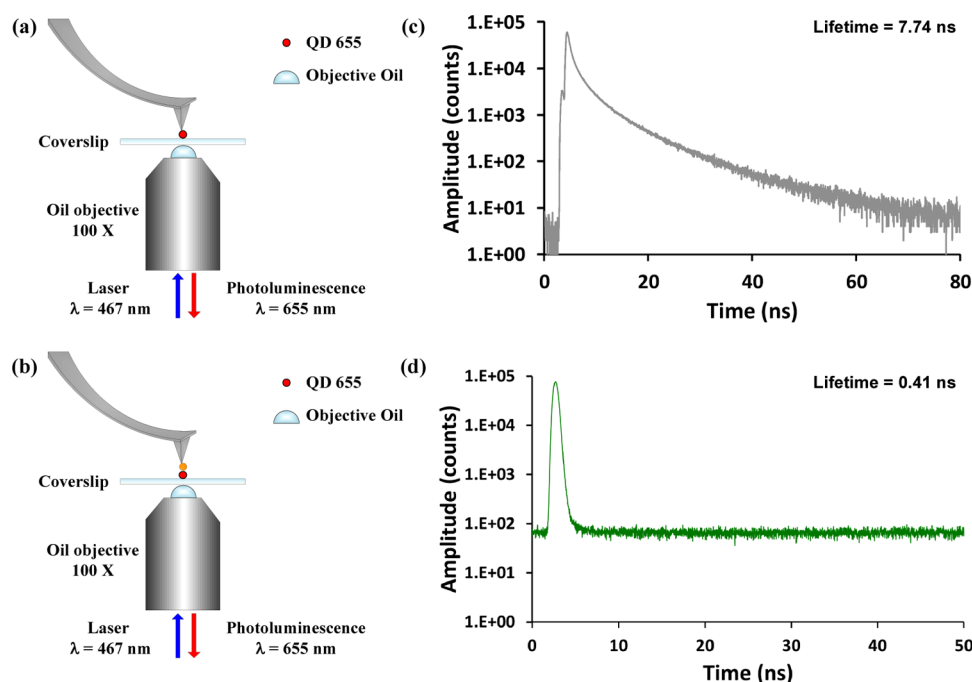
Figure 4. Experimental setup for inspecting fluorescence intensity: single QD on glass coverslip approached by an AFM tip (a) without an Au-NP and (b) with an Au-NP. Corresponding photoluminescence decay times are acquired for setups (c) without and (d) with an Au-NP.
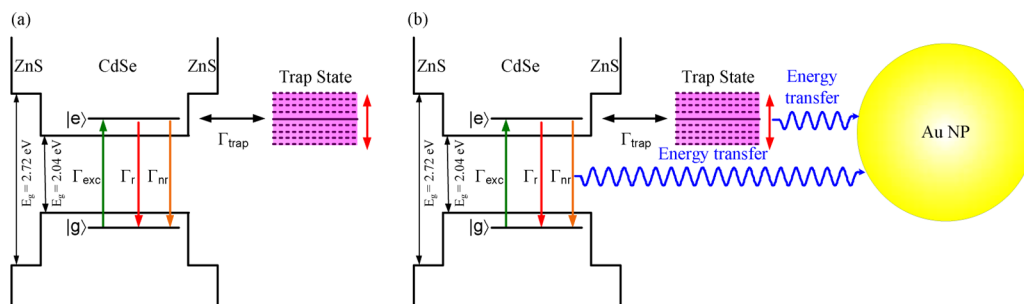

Figure 5. Schematic presentation of various relaxation paths of the following: (a) photoexcited pristine CdSe-ZnS QD; (b) photoexcited CdSe-ZnS QD in the presence of Au-NP.

and leave a ratio of 2/3 of survival rate. In Figure 3c, the 15−20 Å amorphous material coated on the outer surface of the tip and the Au-NP is mostly polymerized hydrocarbon material produced by the electron beam.

The AFM tip with attached Au-NP was used to study the blinking behavior and fluorescence lifespan of a single QD, as shown in Figure 4. Single QD samples were prepared by spin coating a 0.1 nM solution of Qdot 655 on a fused silica substrate. The surface roughness of the fused silica was verified at less than 2 nm (root mean squared value). The fluorescence of a single QD was monitored using a far-field laser scanning confocal microscope for two different cases: in the presence of an AFM tip without (Figure 4a) and with (Figure 4b) an Au-NP. Both cases show blinking-suppression phenomena (data not shown here). The fluorescence lifespan of a single QD when approaching the tip with Au-NP was 1 order of magnitude shorter than that without an Au-NP (from 7.74 to 0.41 ns). When the AFM tip with attached Au-NP approached the QD (Figure 4b), the blinking behavior was significantly suppressed. This was accompanied by fluorescence intensity quenching and lifetime shortening, both of which are typical phenomena associated with a single QD in the proximity of an

Au-NP. These results support the existence of an Au-NP on the tip of the AFM probe.

Fluorescence blinking is the intermittent emission of light produced by a single colloidal QD under continuous excitation. Thus, the fluorescence time trajectory (fluorescence intensity as a function of observation time) alternatively exhibits bright and dark periods. As a matter of fact, identifying the exact mechanism associated with fluorescence blinking remains a matter of debate. Nonetheless, we are certain that charge trapping is a precondition in the formation of blinking dark state. Qdot 655 ITK organic quantum dots are CdSe/ZnS core/shell QDs. In a pristine QD (Figure 5a, in which the QD is not interacting with Au-NP), the bright QD becomes dark when a photoexcited carrier is trapped. The trapped energy itself diffuses over time, transitioning to and from the trap (at a rate Γ_{trap}) only when the trapped energy conforms with a given electronic level alignment. As shown in Figure 5a, upon excitation of the photons, three possible pathways exist through which a single QD may transition from its excited state: (1) radiative recombination (rate Γ_r), (2) nonradiative relaxation (rate Γ_{nr}), and (3) charge trapping (rate Γ_{trap}). As mentioned previously, only charge trapping is capable of inducing
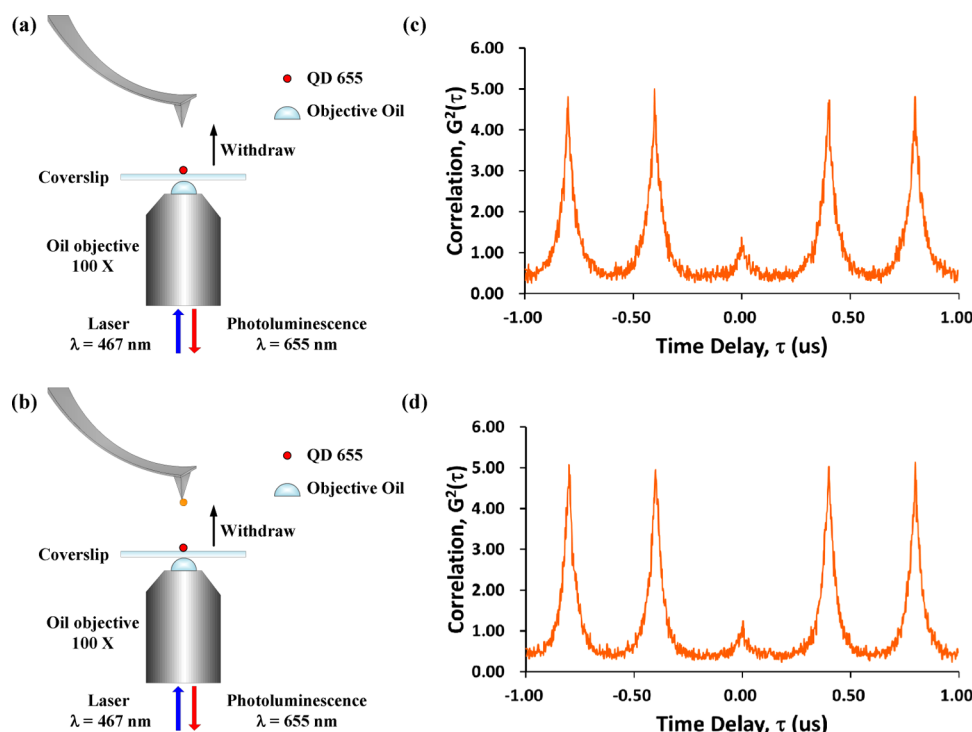
Figure 6. Experimental setup for the analysis of photon antibunching: (a) following withdrawal of the AFM tip without an Au-NP, leaving a single QD on the glass coverslip; (b) following withdrawal of the AFM tip with an Au-NP, leaving a single QD on glass coverslip. Photon antibunching results in (c) and (d) are for the situations in (a) and (b), respectively.

fluorescence blinking. In this case, the blinking rate can be expressed using the following equation:[31]

$$\Gamma_{\text{blinking}} = \frac{\Gamma_{\text{exc}}\Gamma_{\text{trap}}}{\Gamma_{\text{r}} + \Gamma_{\text{nr}} + \Gamma_{\text{trap}}}$$

The blinking behavior of QDs is based on a three-level model, through Auger relaxation of charge carriers, the transient trapping of charge carriers in surface defect states, or both.[32]

Moving metal nanoparticles into the proximity of single QDs can significantly enhance radiative and nonradiative decay rates. Nonradiative decay can be induced through the transfer of energy (dipole−dipole) from a single QD to metal nanoparticles. Radiative decay rates can be increased by increasing the local density of optical states (LDOS). The interplay between single QDs and metal nanoparticles is highly complex and depends on numerous factors, such as the distance separating QDs and metal nanoparticles, relative dipole orientation, and spectral overlap. Generally, the enhancement of the radiative decay rate is similar to that of the excitation rate (Γ_{exc}),[33] assuming that the trapping rate is not influenced significantly by metal nanoparticles. In a small separation regime ($\lesssim 5$ nm) such as the experimental conditions in this study, the rate of nonradiative energy transfer would prevail over the radiative decay rate ($\Gamma_{\text{nr}} \gg \Gamma_{\text{r}}$), thereby dominating the overall decay process leading to the quenching of fluorescence.[34] In this situation, the blinking rate (see the equation above) would be significantly reduced.

After measuring the lifespan of fluorescence, the AFM probe was withdrawn to leave the QD on the coverslip. We then performed photon antibunching analysis, which is the most straightforward means to prove the existence of a single QD in the target position. The results of photon antibunching analysis are presented in Figure 6 and indicate that single QD situation really existed in both experiments.

Photon antibunching is a hallmark of single photon sources. A single photon source means that a light source can emit one and only one photon at a time when it is triggered. This photon antibunching signature is observable in the second-order correlation function obtained using the Hanbury−Brown and Twiss interferometer. A single colloidal CdSe/ZnS QD is a single-photon source because of its atomic-like electronic states.

Figure 7 shows the fluorescence intensity as a function of the distance between the tip with an Au-NP and the QD. At $d = 0$ (Au-NP contacts with QD), the fluorescence intensity measured $\sim$1.5 counts/ms. When the distance decreased to less than 10 nm, the suppression of blinking became significant.

The fluorescence of colloidal QDs can be quenched in the proximity of Au-NPs. The photon count is a function of the
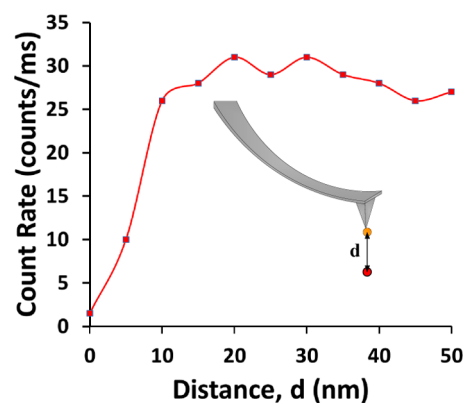

Figure 7. Fluorescence count rate as a function of the distance between the tip with Au-NP and the QD.

distance separating QDs and Au-NPs. Clearly, the intensity of fluorescence is reduced when the distance is smaller than ~10 nm, which is consistent with the results in a previous report.[35,36] Beyond ~15 nm, the intensity of fluorescence is maintained. This is to be expected because the characteristic length for both types of energy transfer (nanometal surface energy transfer, NSET, and fluorescence resonance energy transfer, FRET) is smaller than ~15 nm.

CONCLUSIONS

This paper outlines the methodology used to pick up a single 13 nm Au-NP on the tip of an AFM probe, through the application of electrical bias (greater than 4 V) between the AFM tip and the Au-NP. TEM micrographs and results of fluorescence inspection verify that the Au-NP was secured at the apex of the probe. This paper also discusses Coulomb interaction induced by the tip bias as a possible mechanism underlying the adhesion characteristics observed in these experiments. This is a robust method for the attachment of Au-NPs on the tip of an AFM probe, with a ratio of 2/3 of survival rate.

ASSOCIATED CONTENT

ⓢ Supporting Information

AFM images for picking up Au-NPs of two other sizes (27 and 2 nm) and convolution effect of the tip before and after the attachment of an Au-NP on the AFM tip. This material is available free of charge via the Internet at http://pubs.acs.org.

AUTHOR INFORMATION

Corresponding Author

*Address: Department of Engineering and System Science, National Tsing Hua University, 101, Sec. 2, Kuang Fu Road, Hsinchu 30043, Taiwan, R.O.C. Phone: 886-3-5715131, extension 34270. Fax: 886-3-5720724. E-mail: fangang@ess.nthu.edu.tw.

Present Address

[%]Institute of Cellular and Organismic Biology, Academia Sinica, Taipei 11529, Taiwan.

Notes

The authors declare no competing financial interest.

ACKNOWLEDGMENTS

REFERENCES

(1) Binnig, G.; Rohrer, H.; Gerber, C.; Weibel, E. Surface Studies by Scanning Tunneling Microscopy. *Phys. Rev. Lett.* **1982**, *49*, 57−61.

(2) Binnig, G.; Quate, C. F.; Gerber, C. Atomic Force Microscope. *Phys. Rev. Lett.* **1986**, *56*, 930−933.

(3) Xie, X. N.; Chung, H. J.; Sow, C. H.; Wee, A. T. S. Nanoscale Materials Patterning and Engineering by Atomic Force Microscopy Nanolithography. *Mater. Sci. Eng., R* **2006**, *54*, 1−48.

(4) Gan, Y. Invited Review Article: A Review of Techniques for Attaching Micro- and Nanoparticles to a Probe's Tip for Surface Force and Near-Field Optical Measurements. *Rev. Sci. Instrum.* **2007**, *78*, 081101/1−081101/8.

(5) Ducker, W. A.; Senden, T. J.; Pashley, R. M. Measurement of Forces in Liquids Using a Force Microscope. *Langmuir* **1992**, *8*, 1831−1836.

(6) Ducker, W. A.; Senden, T. J.; Pashley, R. M. Direct Measurement of Colloidal Forces Using an Atomic Force Microscope. *Nature* **1991**, *353*, 239−241.

(7) Mak, L. H.; Knoll, M.; Weiner, D.; Gorschluter, A.; Schirmeisen, A.; Fuchs, H. Reproducible Attachment of Micrometer Sized Particles to Atomic Force Microscopy Cantilevers. *Rev. Sci. Instrum.* **2006**, *77*, 0461041/1−0461041/3.

(8) Lantz, M. A.; Jarvis, S. P.; Tokumoto, H. High Resolution Eddy Current Microscopy. *Appl. Phys. Lett.* **2001**, *78*, 383−385.

(9) Berdyyeva, T. K.; Woodworth, C. D.; Sokolov, I. Human Epithelial Cells Increase Their Rigidity with Ageing in Vitro: Direct Measurements. *Phys. Med. Biol.* **2005**, *50*, 81−92.

(10) Clark, S. C.; Walz, J. Y.; Ducker, W. A. Atomic Force Microscopy Colloid−Probe Measurements with Explicit Measurement of Particle−Solid Separation. *Langmuir* **2004**, *20*, 7616−7622.

(11) Yapici, M. K.; Zou, J. Microfabrication of Colloidal Scanning Probes with Controllable Tip Radii of Curvature. *J. Micromech. Microeng.* **2009**, *19*, 105021/1−105021/9.

(12) Ong, Q. K.; Sokolov, I. Attachment of Nanoparticles to the AFM Tips for Direct Measurements of Interaction between a Single Nanoparticle and Surfaces. *J. Colloid Interface Sci.* **2007**, *310*, 385−390.

(13) Vakarelski, I. U.; Brown, S. C.; Moudgil, B. M. Nanoparticle-Terminated Scanning Probe Microscopy Tips and Surface Samples. *Adv. Powder Technol.* **2007**, *18*, 605−614.

(14) Vakarelski, I. U.; Higashitani, K. Single-Nanoparticle-Terminated Tips for Scanning Probe Microscopy. *Langmuir* **2006**, *22*, 2931−2934.

(15) Wang, H. T.; Tian, T.; Zhang, Y.; Pan, Z. Q.; Wang, Y.; Xiao, Z. D. Sequential Electrochemical Oxidation and Site-Selective Growth of Nanoparticles onto AFM Probes. *Langmuir* **2008**, *24*, 8918−8922.

(16) Okamoto, T.; Yamaguchi, I. Photocatalytic Deposition of a Gold Nanoparticle onto the Top of a SiN Cantilever Tip. *J. Microsc.* **2001**, *202*, 100−103.

(17) Hoshino, K.; Turner, T. C.; Kim, S.; Gopal, A.; Zhang, X. J. Single Molecular Stamping of a Sub-10-nm Colloidal Quantum Dot Array. *Langmuir* **2008**, *24*, 13804−13808.

(18) Eckel, R.; Walhorn, V.; Pelargus, C.; Martini, J.; Enderlein, J.; Nann, T.; Anselmetti, D.; Ros, R. Fluorescence-Emission Control of Single CdSe Nanocrystals Using Gold-Modified AFM Tips. *Small* **2007**, *3*, 44−49.

(19) Lee, S. Y.; Nakaya, K.; Hayashi, T.; Hara, M. Quantitative Study of the Gold-Enhanced Fluorescence of CdSe/ZnS Nanocrystals as a Function of Distance Using an AFM Probe. *Phys. Chem. Chem. Phys.* **2009**, *11*, 4403−4409.

(20) Yuan, C. T.; Yu, P.; Ko, H. C.; Huang, J.; Tang, J. Antibunching Single-Photon Emission and Blinking Suppression of CdSe/ZnS Quantum Dots. *ACS Nano* **2009**, *3*, 3051−3056.

(21) Ritter, C.; Heyde, M.; Schwarz, U. D.; Rademann, K. Controlled Translational Manipulation of Small Latex Spheres by Dynamic Force Microscopy. *Langmuir* **2002**, *18*, 7798−7803.

(22) Liu, Z.; Li, Z.; Wei, G.; Song, Y.; Wang, L.; Sun, L. Manipulation, Dissection, and Lithography Using Modified Tapping Mode Atomic Force Microscope. *Microsc. Res. Tech.* **2006**, *69*, 998−1004.

(23) Suenne, K.; Shafiei, F.; Ratchford, D.; Li, X. Controlled AFM Manipulation of Small Nanoparticles and Assembly of Hybrid Nanostructures. *Nanotechnology* **2011**, *22*, 115301/1−115301/6.

(24) Schäffer, T. E. *High-Speed Atomic Force Microscopy of Biomolecules in Motion in Force Microscopy: Applications in Biology*

and Medicine; Bhanu, P. J., Heinrich Hörber, J. K., Eds; Wiley-Liss: NJ, 2006; pp 221−247.

(25) Santos, S.; Barcons, V.; Christenson, H. K.; Font, J.; Thomson, N. H. The Intrinsic Resolution Limit in the Atomic Force Microscope: Implications for Heights of Nano-Scale Features. *PLoS One* **2011**, *6*, e23821/1−e23821/7.

(26) Xu, J.; Kwak, K. J.; Lee, J. L.; Agarwal, G. Lifting and Sorting of Charged Au Nanoparticles by Electrostatic Forces in Atomic Force Microscopy. *Small* **2010**, *6*, 2105−2108.

(27) Takahashi, K.; Kajihara, H.; Urago, M.; Saito, S.; Mochimaru, Y.; Onzawa, T. Voltage Required To Detach an Adhered Particle by Coulomb Interaction for Micromanipulation. *J. Appl. Phys.* **2001**, *90*, 432−437.

(28) Saito, S.; Himeno, H.; Takahashi, K. Electrostatic Detachment of an Adhering Particle from a Micromanipulated Probe. *J. Appl. Phys.* **2003**, *93*, 2219−2224.

(29) Johnson, K. L.; Kendall, K.; Roberts, A. D. Surface Energy and Contact of Elastic Solids. *Proc. R. Soc. London, Ser. A* **1971**, *324*, 301−313.

(30) Takahashi, K.; Onzawa, T. Simple Formula for the Surface-Energy by a Shifted-Step-Potential Approximation. *Phys. Rev. B* **1993**, *48*, 5689−5691.

(31) Bharadwaj, P.; Novotny, L. Robustness of Quantum Dot Power-Law Blinking. *Nano Lett.* **2011**, *11*, 2137−2141.

(32) Matsumoto, Y.; Kanemoto, R.; Itoh, T.; Nakanishi, S.; Ishikawa, M.; Biju, V. Photoluminescence Quenching and Intensity Fluctuations of CdSe-ZnS Quantum Dots on an Ag Nanoparticle Film. *J. Phys. Chem. C* **2007**, *112*, 1345−1350.

(33) Bharadwaj, P.; Deutsch, B.; Novotny, L. Optical Antennas. *Adv. Opt. Photonics* **2009**, *1*, 438−483.

(34) Kuhn, S.; Hakanson, U.; Rogobete, L.; Sandoghdar, V. Enhancement of Single-Molecule Fluorescence Using a Gold Nanoparticle as an Optical Nanoantenna. *Phys. Rev. Lett.* **2006**, *97*, 017402/1−017402/4.

(35) Yun, C. S.; Javier, A.; Jennings, T.; Fisher, M.; Hira, S.; Peterson, S.; Hopkins, B.; Reich, N. O.; Strouse, G. F. Nanometal Surface Energy Transfer in Optical Rulers, Breaking the FRET Barrier. *J. Am. Chem. Soc.* **2005**, *127*, 3115−3119.

(36) Jennings, T. L.; Singh, M. P.; Strouse, G. F. Fluorescent Lifetime Quenching Near *d* = 1.5 nm Gold Nanoparticles: Probing NSET Validity. *J. Am. Chem. Soc.* **2006**, *128*, 5462−5467.